Protein diffusion in charged polyacrylamide gels
Visualization and analysis

Rebecca K. Lewus, Giorgio Carta*

Department of Chemical Engineering, Thornton Hall, University of Virginia, Charlottesville, VA 22903-2442, USA

Abstract

Protein diffusion in anionic, cross-linked polyacrylamide-based gels supported in fused-silica capillaries was characterized by a direct visualization method. Microphotography was used to obtain transient protein concentration profiles in these gels using cytochrome c as a probe molecule. Gels based on acrylamido-methylpropane sulfonic acid with 2.5–10% N,N'-methylene-bisacrylamide as a cross-linker and with a total polymer concentration of 0.21 g/cm^3 yielded diffuse protein concentration profiles which were quantitatively consistent with a Fickian diffusion model. An analytical method was developed to calculate the diffusivity as a function of protein concentration in the gel from the experimental profiles. The diffusivity was found to assume values in the range 2.5–5.5·10^{-8} cm^2/s and varied somewhat with the protein concentration in the gel. The effects of some of the polymer properties, such as cross-link density, polymer concentration and charge, were also investigated for a limited range of conditions to derive qualitative trends. Results showed that the transport rates increased with a decrease in the cross-link density, were extremely reduced when the polymer concentration was doubled, and were slightly increased when the charge density was decreased by half by polymerizing a 1:1 mixture of acrylamide and acrylamido-methylpropane sulfonic acid monomers. © 1999 Elsevier Science B.V. All rights reserved.

Keywords: Diffusion; Polymer gels; Proteins

1. Introduction

Neutral polymer hydrogels have numerous applications in areas such as size-exclusion chromatography, gel electrophoresis, membrane separations, and drug delivery as a result of their ability to selectively allow molecules to enter and diffuse based on their effective molecular size [1–3]. By introducing a functionality in the polymer network, charged groups, for example, polymer hydrogels can also be used as adsorptive media to effect separations based on charge and/or specific affinity [4–6]. In this case, partitioning and diffusion of molecules through the gel network is affected by both steric and electrostatic phenomena [7,8]. Their hydrophilic character makes such gels ideal for protein separations under non-denaturing conditions. On the other hand, these gels, when used in a ''bulk'' form, are compressed at modest pressure gradients and may undergo swelling and shrinking in response to ionic strength and/or pH changes.

In recent years, hydrogels which are stabilized against mechanical and osmotic forces by incorporating them in a porous rigid matrix have been developed [3,4,9]. As noted by Kapur et al. [3], if the pore size of the supporting rigid matrix is much larger than the hydrogel mesh size, the gel network controls partitioning and transport of molecules

---

*Corresponding author. Tel.: +1-804-924-6281; fax: +1-804-982-2658.

E-mail address: gc@virginia.edu (G. Carta)

within the composite medium. Thus, the desirable properties of charged bulk hydrogels can be retained along with the mechanical strength of a rigid medium. Recent commercial developments include composite matrices for ion-exchange chromatography of proteins, known by the trade name HyperD (BioSepra, Marlborough, MA, USA), obtained by incorporating functionalized, polyacrylamide-based hydrogels within the pores of high-porosity silica or ceramic particles [10,11]. These materials have been characterized experimentally by several authors [12–18]. Under conditions inducing a favorable electrostatic interaction between protein molecules and the gel's ionogenic groups, these materials exhibit high equilibrium uptake capacities for proteins (in excess of 200 mg/cm^3) which are typical of gel-type ion exchangers. On the other hand, because of the mechanical stability of the supporting matrix, they can be utilized in packed chromatographic columns at elevated mobile phase velocities [14]. Interestingly, under conditions that suppress electrostatic interactions (e.g., high ionic strength) or when the protein molecules have a net charge of the same sign as the gel, these materials have been shown to effectively exclude high-molecular-mass proteins [16].

Theoretical analyses and models for the description of protein partitioning and transport in these gel-composite materials have also been presented. Based on the chromatographic behavior of columns packed with these materials Farnan et al. [16] concluded that for non-binding conditions partitioning of proteins is consistent with the Ogston model [19,20] while effective diffusivities are consistent with the theoretical relationship developed by Cukier [21] describing hindered diffusion in fibrous gels. A model to describe mass transfer rates in these materials under binding conditions has been advanced by Fernandez and Carta [13] and Weaver and Carta [15]. This model uses a Fickian diffusion approximation where the driving force is expressed in terms of the adsorbed-protein concentration. Lewus and Carta [22] later modified this approach by introducing a Maxwell–Stefan formulation which was shown to be consistent with both single and binary protein uptake data. In either case, the basic premise for these models is that protein molecules retain ''mobility'' within the gel, i.e., that these molecules are not irreversibly bound onto the gel functional groups.

In this paper we report a direct visualization of protein diffusion in charged polyacrylamide-based gels supported in fused-silica capillaries for conditions where a highly favorable partitioning of the protein in the gel occurs as a result of electrostatic interaction. Optically transparent anionic gels are synthesized in situ within small capillary tubes with a square section. Cytochrome *c*, an intensely colored cationic protein, is used as a probe molecule. The evolution of protein concentration profiles within the gel obtained by exposing the capillary-gel composites to a dilute cytochrome *c* solution is followed by direct observation with a microscope. The concentration profiles obtained from a gray-scale analysis of digitized images are then treated numerically to determine the effective protein diffusivity as a function of protein concentration in the gel. The effects of cross-link density, charge density and polymer concentration are investigated for a limited number of cases.

2. Experimental

2.1. Materials

Chemicals used in the preparation of gels were 2-acrylamido-2-methylpropane sulfonic acid (AMPS), *N,N′*-methylene-bisacrylamide (MBA), ammonium persulfate (AP), *N,N,N,N*-tetra-ethylenediamine (TEMED) and acrylamide. These chemicals were obtained from Lancaster (Windham, NH, USA) and Sigma (St. Louis, MO, USA). Bind-silane (γ-methacryloxy-propyl-trimethoxysilane) was obtained from Pharmacia (Piscataway, NJ, USA). Cytochrome *c* from bovine heart (M_r=13 300, isoelectric point, pI=10.6) was obtained from Sigma. Other chemicals were obtained from Sigma or Fisher Scientific (Pittsburgh, PA, USA). Fused silica, polyimide-coated capillary tubing with a square cross-section was obtained from Polymicro Technologies (Phoenix, AZ, USA). The nearly perfect square section of this capillary has an internal width of 100 μm and an external width of 300 μm. The tubing was cut in approximately 1-cm sections and the polymer coating was burned off from the top 0.5–0.6 cm. The sections were then treated with bind-silane following the procedure recommended by the supplier. The bind-silane provides a way of anchoring

the polyacrylamide gel by covalent attachment to the capillary.

2.2. Preparation of gels

Many methods have been used for the synthesis of polyacrylamide-based gels. In this work, we used a modification of the methods described by Girot and Boschetti [10]. For the preparation of 5% cross-linked gels, 2 g of the AMPS monomer and 0.1 g of the cross-linker MBA are added to 5 cm^3 of distilled, filtered, degassed water. The solution is titrated with NaOH to a pH between 6 and 8. The solution volume is then brought to 10 cm^3 with additional degassed water. The initiator AP (0.0005 g) and the promoter TEMED (10 μl) are then added and stirred in the solution. The reaction mixture is then quickly loaded into the capillary sections with a syringe. Polymerization starts 5–10 min after addition of the initiator and promoter at room temperature and appears to be complete (as indicated by the cessation of heat evolution) in about 1 h. Upon completion of the polymerization, the capillary is placed into a large volume of 10 mM Na$_2$HPO$_4$ buffer at pH 6.5 containing 1 mM sodium azide as a bacteriostatic agent and allowed to equilibrate for at least 24 h. The same procedure was followed to prepare gels with different cross-link density and polymer concentration by varying the amounts of the chemicals used. Gels of different charge density were prepared by substituting acrylamide for a fraction of the AMPS monomer.

Microscopic observation of the capillaries after equilibration in buffer revealed that minimal volume change occurred. Moreover, hydraulic pressure testing with a syringe showed that the capillaries were filled with gel which has extremely low hydraulic permeability [23]. The charge density, based on the gel volume, can thus be estimated from the composition of the polymerization mixture. The polymer volume fraction $\phi = m_p v_p/(m_p v_p + m_w v_w)$ was estimated from the initial monomer composition using a value of $v_p = 0.7$ cm^3/g for the polymer density as suggested by Kapur et al. [23]. A charge density of 970 μequiv./cm^3 and a value of $\phi = 0.15$ are obtained for gels prepared as described above. The charge density is higher than the value reported by Kapur et al. [23] for similar charged-gels immobilized in porous membranes. However, the value of ϕ

is essentially the same as that reported by these authors.

2.3. Diffusion measurements

A schematic of the diffusion cell and experimental apparatus used in this work is shown in Fig. 1. The cell was realized by sandwiching a 1/8 in. thick PTFE gasket between two microscope slides (1 in.= 2.54 cm). The end of the capillary tube sections prepared as described above were sealed by gluing them to the tip of a syringe needle with a cyanoacrylate adhesive which was inserted in a hole drilled on the side of the PTFE gasket. The protein solution was allowed to flow in and out of the cell through small stainless steel tubes also inserted through holes drilled in the PTFE gasket and was recirculated to a 20 cm^3 reservoir with a peristaltic pump (Cole-Parmer, Chicago, IL, USA) at a flow-rate of 0.5 cm^3/min. This corresponds to a fluid velocity past the tip of the capillary greater than 120 cm/h. The evolution of concentration profiles in the gel was followed by direct observation with a Bausch and Lomb Balplan microscope at 100× magnification. Images were acquired with a color CCD video camera (Sanyo Model VCC3962) and captured with a Macintosh Performa 636CD computer equipped with a video input board. Cytochrome *c* is intensely colored (reddish-brown) and is very favorably partitioned in these gels at low ionic strength [22]. Thus, diffusional transport of this molecule in the gel can be characterized by direct visual observation. Gray-scale analysis of the digitized images was performed using NIH Image software. The gray scale values were then converted to protein concentration in the gel using a calibration curve obtained by determining the gray scale for identical capillaries filled with cytochrome *c* solutions of different concentrations. As expected, the relationship between protein concentration and color intensity (or gray scale) was found to be non-linear and followed approximately the Beer–Lambert law. Thus, there is a loss of precision in the colorimetric determination of protein profiles which occurs at higher concentrations. The square section capillaries were chosen to eliminate optical artifacts which were observed when using standard round capillaries.

Both uptake (adsorption) and desorption experiments were conducted. Adsorption profiles were

Side View

Top View

Color CCD camera

In-line filter

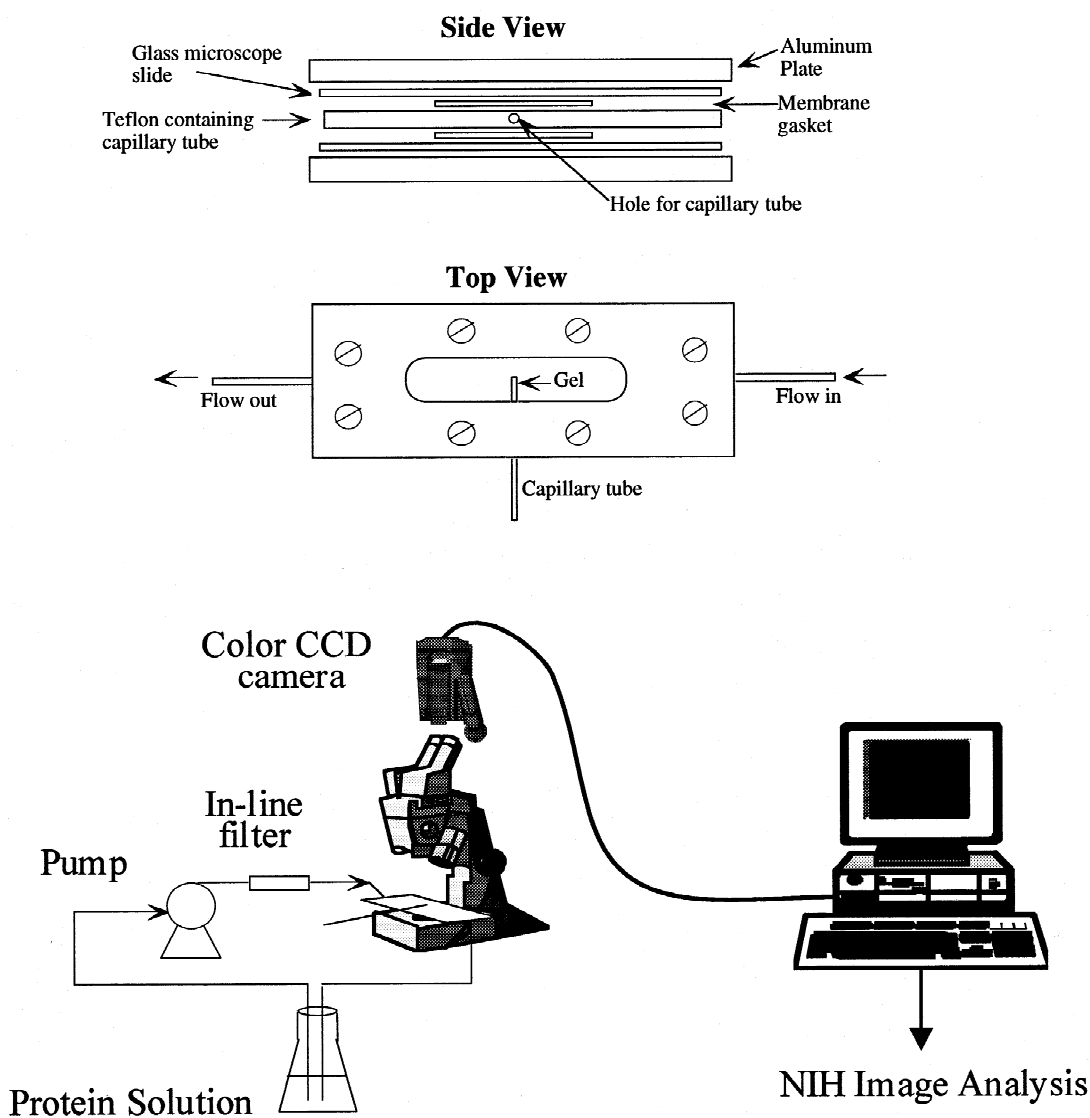**Pump**

Protein Solution

NIH Image Analysis

Fig. 1. Diffusion cell and apparatus for observation of protein concentration profiles in supported gels.

measured starting with clean gel tubes with solutions containing 1 mg/cm^3 cytochrome c in 10 mM Na$_2$HPO$_4$ buffer at pH 6.5. At the end of the adsorption measurement flow to the diffusion cell was switched from the protein solution to a solution containing 500 mM NaCl in pH 6.5 buffer. At this ionic strength, essentially all of the cytochrome c previously adsorbed by the gel was found to be desorbed. This result is consistent with observations by Lewus et al. [24] for adsorption and desorption on

HyperD-type materials. All experiments were conducted at room temperature, 23±2°C.

3. Results

Digitized images of the evolution of cytochrome c concentration profiles during an adsorption experiment are shown in Fig. 2 along with calibrated profiles. In these images, the gray area (red in the
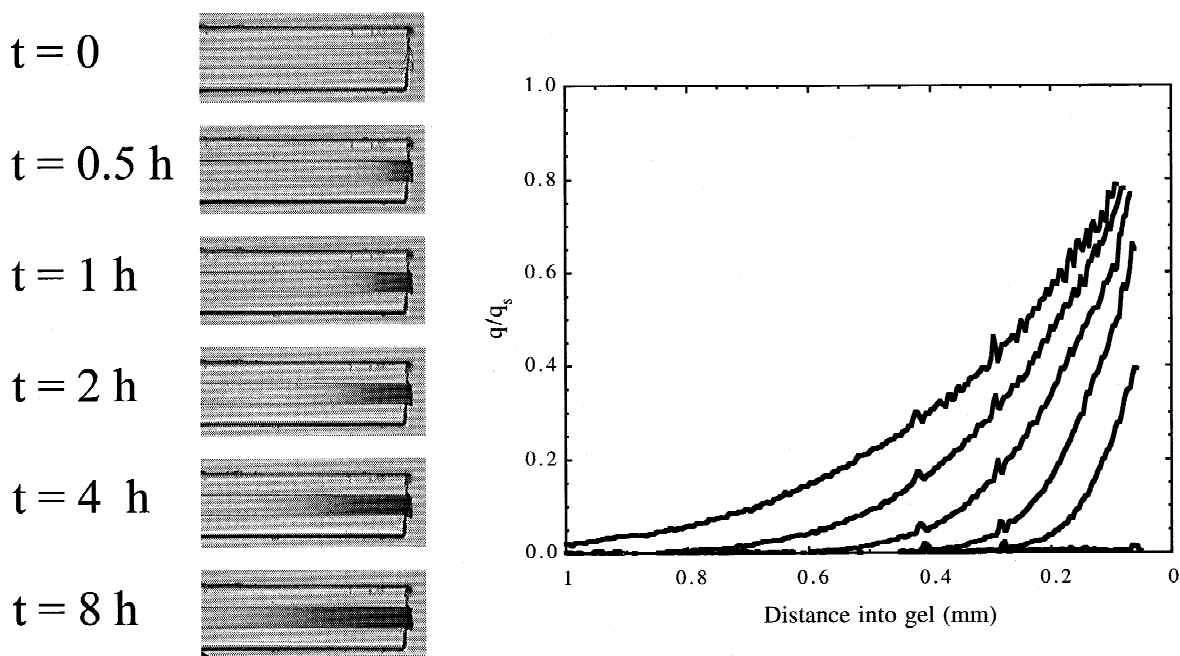
Fig. 2. Gray scale images and digitized concentration profiles for cytochrome c adsorption in a 10% cross-linked gel. Charge density$=970$ μequiv./cm^3, polymer concentration$=0.21$ g/cm^3, $C=1$ mg/cm^3, $q_s=420$ mg/cm^3.

actual image) surrounding the capillary corresponds to the 1 mg/cm^3 cytochrome c solution. The darker gray band seen progressing toward the left represents the cytochrome c penetration in the gel. Because of imperfections near the cut end of the capillary, the concentration profiles could not be followed reliably all the way to the tip and, thus, are omitted from the figure. However, it can be clearly seen both from the images and from the digitized profiles that the cytochrome c band appears to have a smooth, diffuse nature with the concentration gradually declining to a low value from a maximum at the exposed tip of the capillary. As evident from the contrast in gray scale, cytochrome c is partitioned very favorably in the gel phase for these conditions. The equilibrium partitioning of cytochrome c was determined independently by equilibrating samples of the capillary-supported 5% cross-linked gels with a cytochrome c solution and then desorbing the protein in a known volume of 500 mM NaCl buffer. The amount of protein bound was calculated from a material balance based on an analytical determination of the concentration of the desorbed protein in the salt buffer. The latter was determined by measuring the absorbance at 405 nm

with a spectrophotometer (Beckman, Model DU50). These determinations gave a value of $q_s=410\pm80$ mg/cm^3. Similar results were obtained with gels having 2.5 and 10% cross-linking with q_s in the range 390–420 mg/cm^3. It should be noted that these capacity values are lower-bound estimates since it cannot be excluded that a small amount of protein was irreversibly bound and did not come-off when the gels were exposed to the salt solution.

Assuming a value of 0.7 cm^3/g for the specific volume of the protein [25], the measured protein-binding capacity corresponds to a volume fraction of protein in the gel of 0.29 ± 0.06. Although this value may seem high, it is consistent with measurements of protein uptake equilibria in HyperD-type particles. For example, uptake capacities of 150 and 250 mg/cm^3 have been reported for cytochrome c and lysozyme in S-HyperD particles [22]. Since the silica matrix of these particles does not contribute to adsorption and the porosity of the base silica is around 0.6, these values correspond to capacities of 250 and 420 mg/cm^3 when expressed on a gel-volume basis. Differences in the capacity values between the results obtained with our gels and those

obtained with the commercial particles could be caused by differences in the method of synthesis [23] and by the fact that our gels have a greater charge density than the value of 370 μequiv./cm^3 of gel of the commercial S-HyperD materials used by Lewus and Carta [22].

As previously noted, some optical artifacts exist near the tip of the gel and a small amount of gel is seen to protrude slightly into the solution. These artifacts render impossible an accurate determination of the profiles very near the tip. However, since the times of observation are quite long and the depth of penetration of the cytochrome c band is substantial, these imperfections at the boundary should be of limited significance in the interpretation of the results. We also checked for the absence of signifi-cant protein concentration variations in the direction transverse to the capillary. As seen for example in Figs. 2 and 3, the concentration profiles appear to be flat in this direction. From the gray-scale analysis of the digitized images such variations were found to be very small ($<5\%$) except for the region very near the walls where shadowing from the vertical walls of the

capillary prevented an accurate determination of the concentration. These regions, amounting to less than 10% of the total width, were of course not used to calculate the axial concentration profiles.

Digitized images and concentration profiles of cytochrome c in the gel during desorption with 500 mM NaCl following the 8 h of adsorption time of the experiment in Fig. 2 are shown in Fig. 3. The protein concentration in the gel near the exposed tip is rapidly reduced to a low value and the protein is gradually desorbed by diffusing outward. Diffusion toward the unexposed end of the capillary continues, however, resulting in a concentration band which is diffuse at both ends with a maximum in the middle. This maximum moves toward the unexposed end of the gel as desorption continues.

The effects of cross-link density on the evolution of concentration profiles in the gel are shown in Fig. 4 for gels with 2.5 and 10% cross-linking with similar polymer concentration and charge density for both adsorption and desorption conditions. Profiles for 5% cross-linking were also obtained and found to be intermediate between those shown in Fig. 4. For
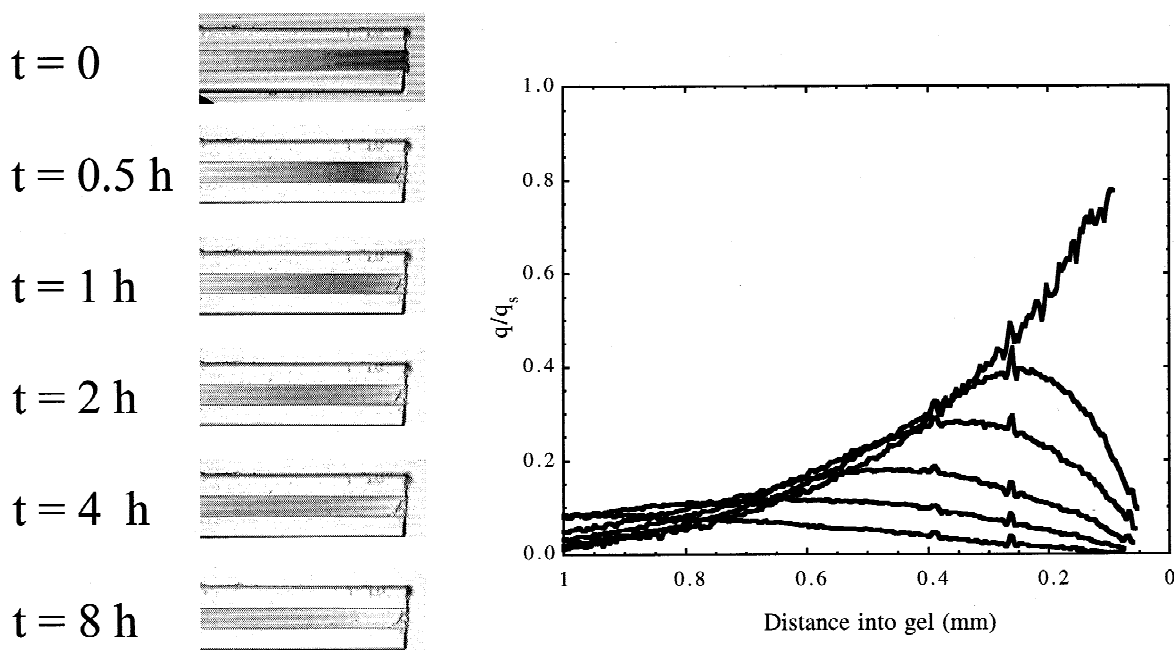

Fig. 3. Gray scale images and digitized concentration profiles for cytochrome c desorption from a 10% cross-linked gel with 500 mM NaCl. Charge density$=970$ μequiv./cm^3, polymer concentration$=0.21$ g/cm^3, $q_s=420$ mg/cm^3.
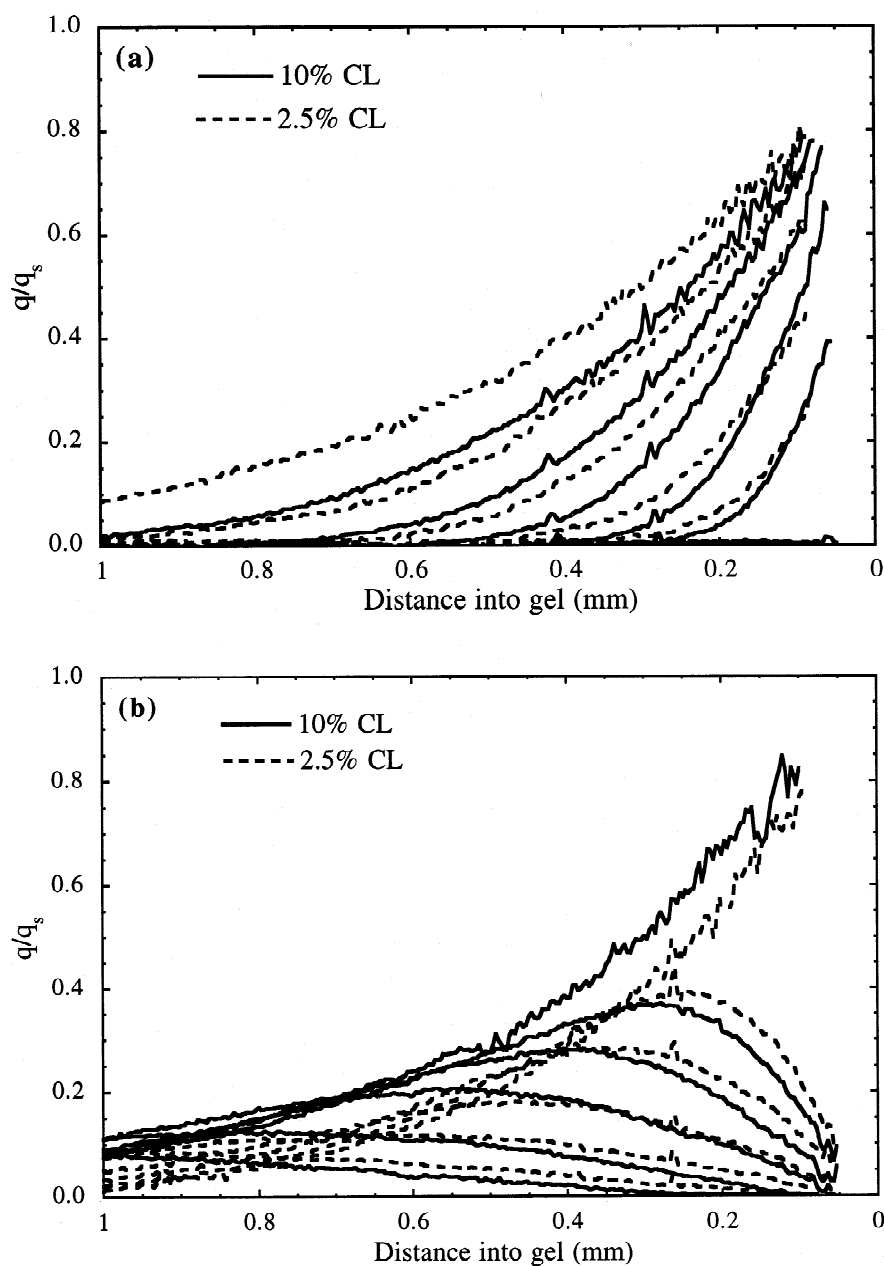
Fig. 4. Comparison of concentration profiles for cytochrome c obtained with 2.5 and 10% cross-linked gels for (a) adsorption and (b) desorption with 500 mM NaCl. Charge density=970 μequiv./cm^3, polymer concentration=0.21 g/cm^3, q_s=390 mg/cm^3 for 2.5% CL, q_s=420 mg/cm^3 for 10% CL. Profiles are shown at 0, 0.5, 1, 2, 4 and 8 h.

clarity, these profiles are omitted from the figure. In all three cases, the maximum cytochrome c concentration in the gel had values in the range 410±80 mg/cm^3. The lower cross-linking gels exhibited

somewhat faster adsorption rates (as evidenced by the greater depth of penetration of the protein profile). However, the difference in transport rates is relatively small. In fact, it is much smaller than could

be expected for free, bulk gels. This can be understood by considering the fact that in our case, the gel volume and, hence, the polymer concentration remain essentially constant being limited by the volume of the supporting capillary. The observation that the volume remains constant was also reached by Kapur et al. [23] for their gels supported in porous matrices. Of course, a rather different result would be obtained for bulk gels since, in that case, varying the cross-link density would have a large effect of the extent of swelling and, thus, on the polymer concentration.

The effect of increasing the polymer concentration is shown in Fig. 5 which compares the results obtained with 5% cross-linked gels with polymer concentrations of 0.21 and 0.42 g/cm^3 for adsorption conditions. It is apparent that increasing the polymer concentration has a profound effect on the rate of diffusion of cytochrome c. A lower value of $q_s \sim 260$ mg/cm^3 is also obtained indicating restricted access of the protein to the polymer network. Finally, Fig. 6 shows the effect of charge density for 5% cross-linked gels for both adsorption and desorption con-

ditions. Similar q_s values and transport rates are obtained in both cases.

4. Discussion

Polymeric gels have a chain-like structure and have been modeled as a network of randomly-oriented straight cylindrical fibers. Models of this type have been used as the basis for the development of theories to predict the effects of gel and solute properties on partitioning and diffusion of neutral molecules [2]. In general, these theories predict that both partitioning and diffusivity decline exponentially with polymer concentration and size of the diffusing molecule. These trends have also been shown to hold for gels supported in rigid matrices [3]. Although some attempts have recently been made to incorporate electrostatic contributions to partitioning of proteins in charged gels [7,8], it is difficult to make a priori predictions for gels such as the ones used in this work where partitioning is extremely favorable. A significant complication is
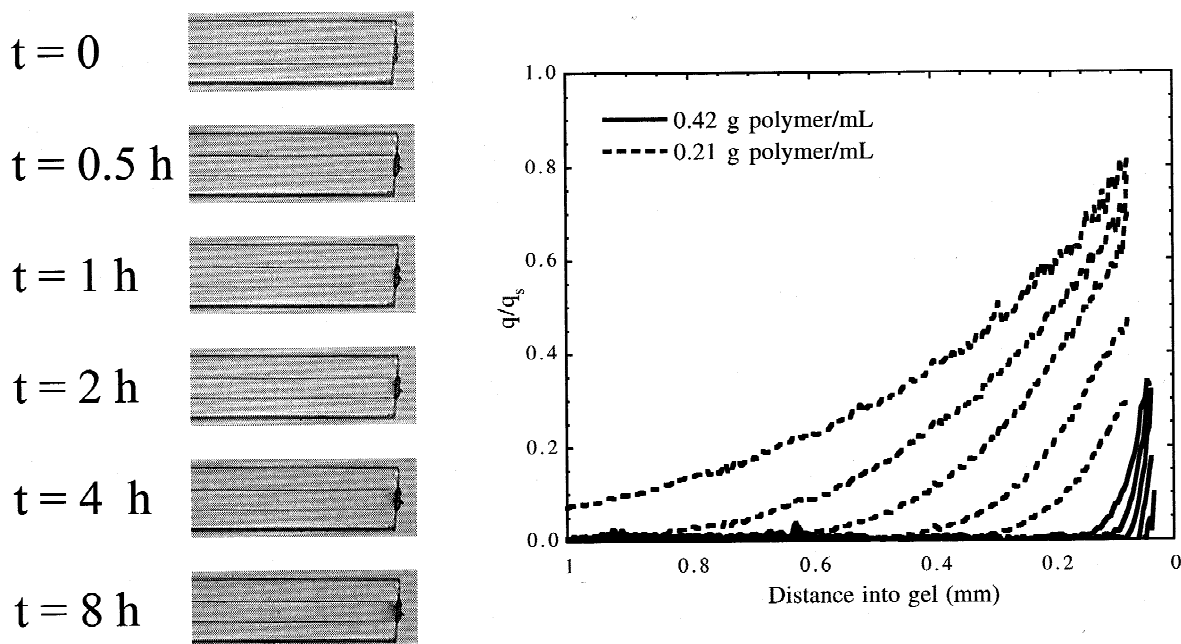

Fig. 5. Comparison of concentration profiles for cytochrome c adsorption obtained with 0.21 and 0.42 g/cm^3 polymer concentration gels. Cross-link density=5%, charge density=970 and 1940 μequiv./cm^3. Images on left shown for 0.42 g/cm^3 gel.
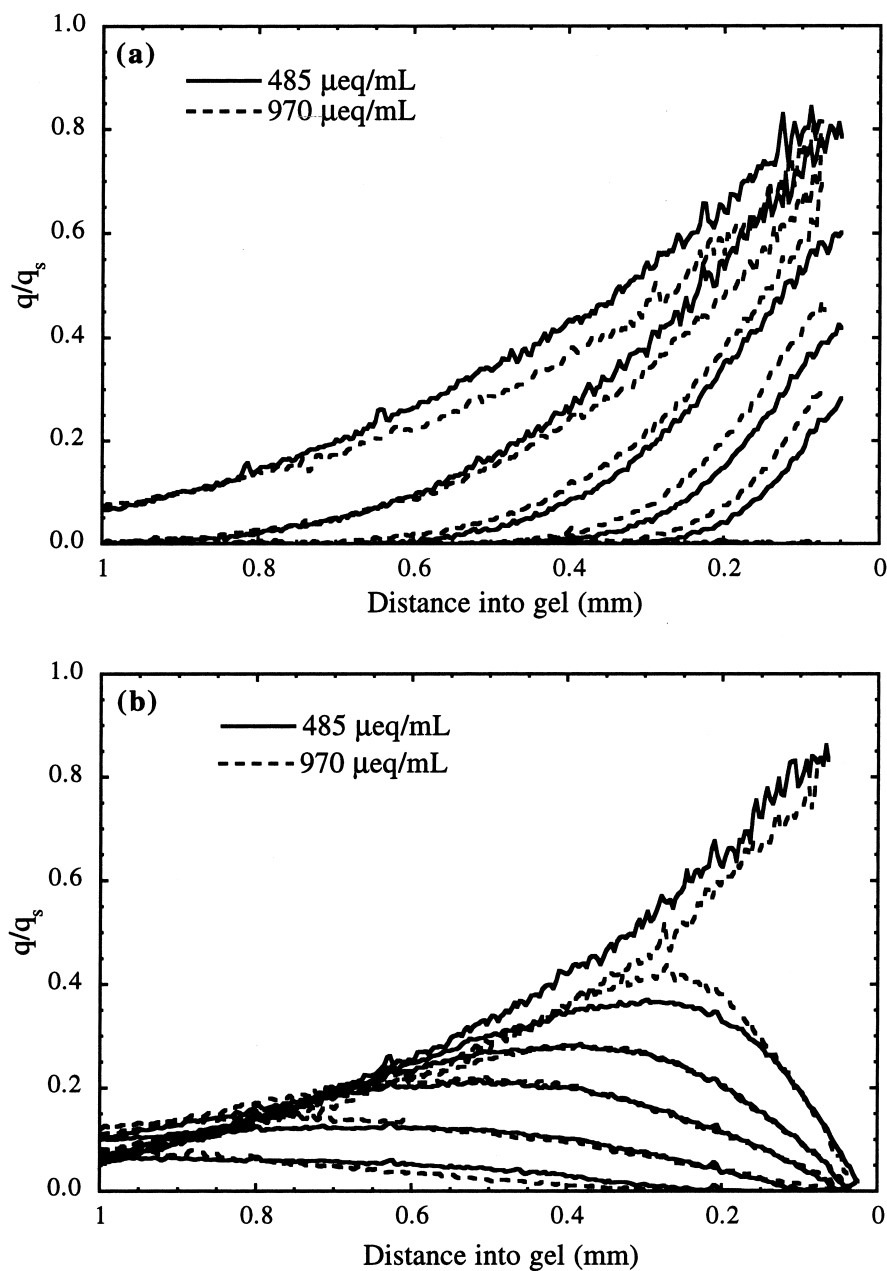
Fig. 6. Comparison of concentration profiles for cytochrome c obtained with 485 and 970 μequiv./cm^3 charge density gels for (a) adsorption and (b) desorption with 500 mM NaCl. Cross-link density = 5%, polymer concentration = 0.21 g/cm^3, q_s = 370 mg/cm^3 for lower charge density gel. Profiles are shown at 0, 0.5, 1, 2, 4 and 8 h.

that solute–solute and solute–gel interactions can make the diffusivity a concentration-dependent quantity.

A mathematical approach can be applied to our concentration profile data to determine an effective diffusion coefficient as a function of protein con-

centration in the gel. Although different models such as the Maxwell–Stefan approach or a Nernst–Planck formulation [26] could be applied, we adopted a simpler ''unstructured'' Fickian diffusion model with a concentration-dependent diffusivity $D_s(q)$. For uniaxial diffusion in a semi-infinite slab of gel initially free of solute, the following equation and boundary conditions can be written:

$$\frac{\partial q}{\partial t} = \frac{\partial}{\partial z}\left[D_s(q)\frac{\partial q}{\partial z}\right] \tag{1}$$

$$t = 0: q = 0 \tag{1a}$$

$$z = 0: q = q_s \tag{1b}$$

$$z \rightarrow \infty: q = 0, \partial q/\partial z = 0 \tag{1c}$$

Inspection of the experimental profiles in Fig. 2, for example, shows that these boundary conditions are compatible with the experimental system. This occurs because equilibrium is achieved rapidly (compared to the time scale of the experiment) at the exposed tip of the capillary and the concentration profile is not allowed to extend to the opposite end.

Applying the Boltzmann transformation to Eq. (1), yields the following ordinary differential equation:

$$-\frac{\eta}{2}\cdot\frac{dq}{d\eta} = \frac{d}{d\eta}\left[D_s(q)\frac{dq}{d\eta}\right] \tag{2}$$

where:

$$\eta = \frac{z}{\sqrt{t}} \tag{3}$$

Finally, integrating Eq. (2) from $\eta = \infty$ to η yields:

$$D_s(q) = \frac{-\int_0^q \eta\,dq}{2\left(\dfrac{dq}{d\eta}\right)_q} \tag{4}$$

Thus, the diffusivity can be determined as a function of concentration directly from the concentration profiles. As an example, Fig. 7 shows the data of Fig. 2 plotted as a function of η for times of 1–8 h. The region near the exposed tip of the capillary is omitted from this graph and was not used to calculate the diffusivity since this region is affected by optical artifacts. The collapse of the profiles for different times onto a single curve supports the
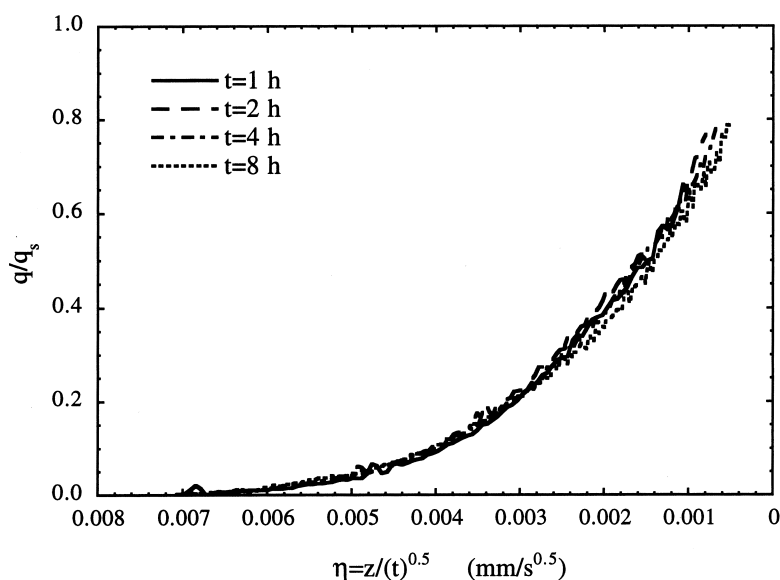

Fig. 7. Concentration profiles for cytochrome c adsorption in a 10% cross-linked gel plotted as a function of η. Conditions as in Fig. 2.

validity of the approach. To carry out the integral and derivative calculations needed for Eq. (4), the experimental profiles at each time in η vs. q form were fitted with a smooth function. Integral and derivative terms were then computed analytically. Calculated diffusivities as a function of protein concentration in the gel using this procedure are summarized in Fig. 8 for gels with 2.5, 5 and 10% cross-linking. The diffusivities are similar for 2.5 and 5% cross-linking but they are significantly lower for 10% cross-linking. In all three cases, however, the diffusivity varies somewhat with protein concentration in the gel. It should be noted that although the diffusivity values obtained experimentally are much lower than the free solution diffusivity of cytochrome c ($D_0 \sim 1 \cdot 10^{-6}$ cm^2/s), the mass transfer flux is much higher than could be predicted for fluid-phase diffusion of free protein. Since in Eq. (1) the flux is expressed with a driving force written in

terms of the adsorbed-protein concentration, an equivalent effective diffusivity, $\tilde{D}_e$, based on a fluid-phase driving force can be calculated as [15]:

$$\tilde{D}_e \sim D_s \times \frac{q_s}{C} \qquad (5)$$

where q_s/C is the partition ratio. For our experimental conditions $q_s/C \sim 410$. Thus, the equivalent diffusivity values are in the range 1.1–$1.3 \cdot 10^{-5}$ cm^2/s for the 10% cross-linked and increase to the range 1.8–$2.3 \cdot 10^{-5}$ cm^2/s for the 2.5% cross-linked gel. Since the equivalent effective diffusivity values are more than 10-times larger than the free solution diffusivity, transport through the adsorbing gel for these conditions is many times faster than could be predicted for diffusion in the liquid phase. This result is qualitatively consistent with observations of Fernandez and Carta [13] and Weaver and Carta [15] who have reported high rates of mass transfer of
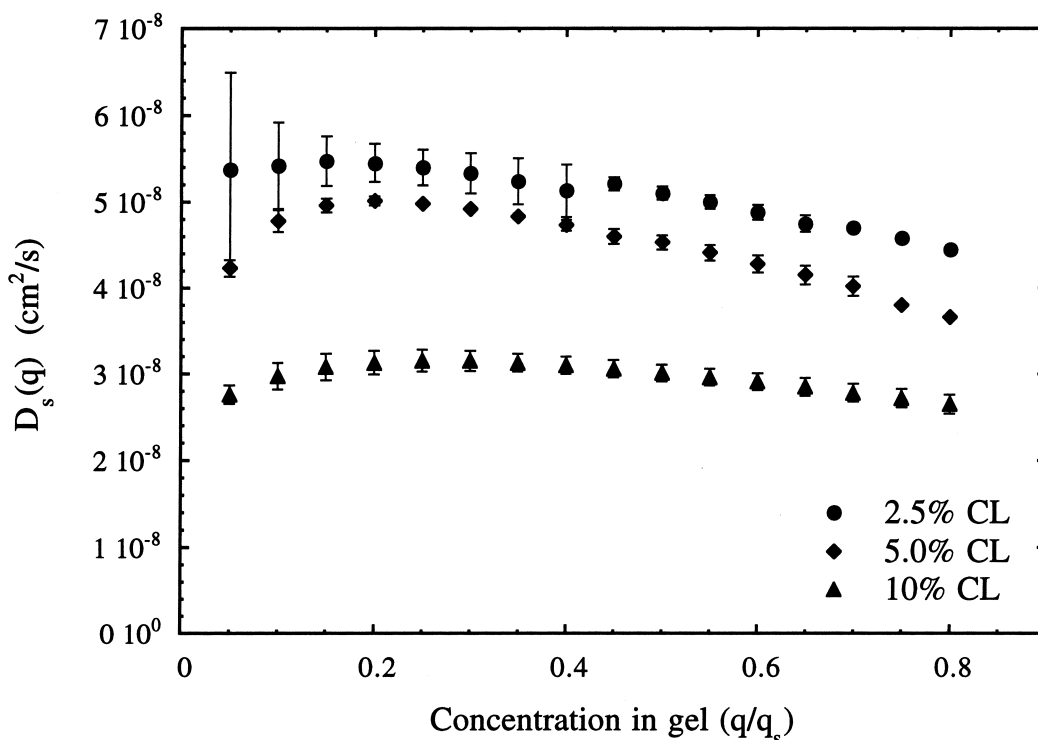

Fig. 8. Calculated diffusivity for cytochrome c in gels with 2.5, 5 and 10% cross-linking. Error bars represent ±one standard deviation for determinations using concentration profiles at 1, 2 and 4 h.

proteins in HyperD particles under favorable binding conditions. Although lower diffusivity values were found in those studies, this is to be expected since porosity and tortuosity factor corrections should apply for transport in gels contained in porous particles such as HyperD.

A final consideration regards the ability to predict adsorption and desorption profiles using the diffusivity data in Fig. 8. For this purpose, these data were fitted empirically with a quadratic function over the range of $q/q_s = 0$–0.8 and extrapolated to values of $q/q_s = 1$. Since the diffusivity was relatively constant, the slight extrapolation appears to be reasonable. A numerical solution of Eq. (1) incorporating this function was then obtained with a finite difference scheme similar to that used by Kataoka et al. [27]. For adsorption, the boundary conditions are those given in Eqs. (1a–1c). To match the boundary conditions at $z \to \infty$ the domain for numerical integration was chosen sufficiently large that increasing it further did not change the computed profiles. The same approach was used for desorption calculations, except that the initial condition was the concentration profile predicted at the end of the adsorption run while the boundary condition was replaced by $q = 0$. As an example, predicted adsorption and desorption profiles are shown in Fig. 9 for the conditions of the experimental runs in Figs. 2 and 3. The agreement with the adsorption profiles is, as expected, very good since the experimental curves at times of 1, 2 and 4 h were used to generate the diffusivity data. However, the model also predicts the profiles at 0.5 and 8 h which were not used to determine D_s. Predictions of the desorption profiles are also quite reasonable but not completely quantitative. The model appears to underpredict somewhat the diffusion rates although the general shape of the curves is reproduced. In particular, there is agreement with the general location of the concentration maximum and with the continuous development of concentration profiles inward, away from the exposed tip of the gel-filled capillary tube. Lewus et al. [24] have also attempted to predict desorption curves in HyperD media using diffusivity values obtained under adsorption conditions. The results in that case also indicated that somewhat higher diffusivities were needed to predict the rate of desorption. Results similar to those shown in Fig. 9 were also obtained for gels with 2.5 and 5% cross-linking.

5. Conclusions

Direct observation of protein concentration profiles in charged polyacrylamide gels supported in a capillary tubes provides important insight regarding the diffusion mechanism and the transport rates of proteins which are electrostatically bound under both adsorption and desorption conditions. Firstly, this work further confirms that supported gels which are stabilized against deformations induced by mechanical and osmotic forces can be produced by synthesizing them in situ within a rigid matrix. Silanizing the walls of fused-silica capillaries ensures a stable structure that exhibits minimal volume change after polymerization. A highly favorable partitioning of proteins with charge opposite to that of the gel is observed in such structures at low ionic strength. Secondly, it is apparent that smooth, diffuse protein concentration profiles are established within the gel under adsorption conditions. These profiles progress gradually into the gel until complete saturation. Smooth profiles are also obtained when adsorbed protein is desorbed by contact with a high ionic strength solution. If only diffusion of ''free'' protein occurred, a sharp transition between a region of complete saturation and a shrinking clean core would be expected. Thirdly, it appears that the concentration profiles are not only qualitatively but also quantitatively consistent with a Fickian diffusion model where the flux is proportional to a driving force expressed in terms of the adsorbed-protein concentration in the gel. The corresponding diffusivity, however, varies somewhat with protein concentration in the gel. Finally, we observed the effects of some of the gel properties on the rates of mass transfer. The rates decrease with an increase in the cross-link density, increase slightly by halving the charge density, and are dramatically reduced by doubling the polymer concentration in the supported gel.

In conclusion, it should be noted that Fickian diffusion models invoking ''surface'' or ''solid-phase'' diffusion or parallel contributions of ''surface'' diffusion and ''pore'' diffusion of free protein molecules have been assumed either explicitly or implicitly by many different authors to describe mass transfer of proteins in various ion exchangers under adsorbing conditions, e.g., [17,18,28–33]. While such models often provide a consistent correlation of
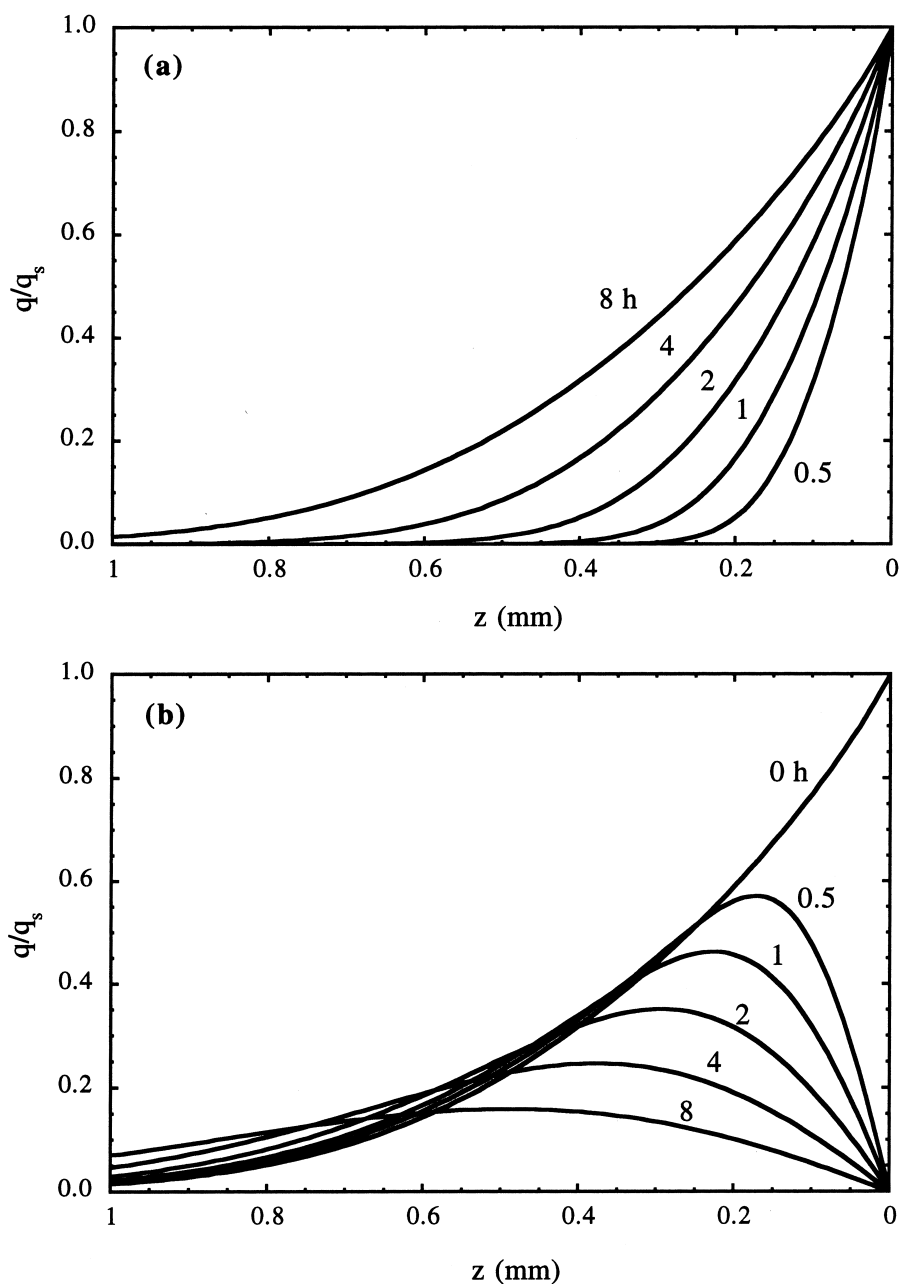
Fig. 9. Predicted concentration profiles for (a) adsorption and (b) desorption of cytochrome *c* from a 10% cross-linked gel from the numerical solution of Eq. (1). Simulated conditions are the same as in Figs. 2 and 3.

experimental results and have been proven extensively for diffusion of small molecules in various adsorbents and ion exchangers, e.g., [26,34], to our knowledge there has been no direct demonstration of their validity for macromolecules. In our case, since

protein binding is extremely favorable for the conditions studied, if diffusion of unbound protein were solely responsible for intraparticle transport, concentration profiles much sharper than those seen experimentally would be observed. The experimental

profiles reported in this paper, thus, provide strong evidence to support a model for macromolecule transport in charged gels where the flux is driven by a gradient in adsorbed-phase concentration. The combination of highly favorable partitioning and sufficiently high mobility results in mass transfer rates higher than could be observed by diffusion of free protein alone. The diffusivity in such models should, however, generally be considered a function of concentration. Extension of these measurements to multicomponent transport should be feasible with our experimental approach and will be the subject of a future communication.

6. Nomenclature

C	protein concentration in solution, mg/cm^3
D_0	free solution diffusivity, cm^2/s
$\tilde{D}_e$	equivalent diffusivity based on a fluid-phase driving force, cm^2/s
D_s	diffusivity based on an adsorbed-phase driving force, cm^2/s
q	protein concentration in gel, mg/cm^3
q_s	saturation protein concentration in gel, mg/cm^3
m_p	mass of polymer in gel, g
m_w	mass of water in gel, g
t	time, s
v_p	specific volume of polymer in gel, cm^3/g
v_w	specific volume of water in gel, cm^3/g
z	axial coordinate, cm

6.1. Greek symbols

ϕ	volume fraction of polymer in gel
η	Boltzmann transformation variable ($=z/\sqrt{t}$)

Acknowledgement

References

[1] J.A. Wesselingh, J. Control. Rel. 24 (1993) 47–60.

[2] E.M. Johnson, D.A. Berk, R.K. Jain, W.M. Deen, Biophys J. 70 (1996) 1017–1026.

[3] V. Kapur, J. Charkoudian, J.L. Anderson, J. Membr. Sci. 131 (1997) 143–153.

[4] E. Boschetti, J. Chromatogr. A 658 (1994) 207–236.

[5] S.H. Gehrke, E.L. Cussler, Chem. Eng. Sci. 44 (1989) 559–566.

[6] E. Kokufuta, E. Jinbo, Macromolecules 25 (1992) 3549–3552.

[7] E.M. Johnson, W.A. Deen, J. Coll. Int. Sci. 178 (1996) 749–756.

[8] A.P. Sassi, H.W. Blanch, J.M. Prausnitz, AIChE J. 42 (1996) 2335–2353.

[9] J. Tong, J.L. Anderson, Biophys. J. 70 (1996) 1505–1513.

[10] P. Girot, E. Boschetti, US Pat., 5 268 097 (1993).

[11] E. Boschetti, L. Guerrier, P. Girot, J. Horvath, J. Chromatogr. B 664 (1995) 225–231.

[12] A.E. Rodrigues, J.C. Lopes, C. Chenou, R. de la Vega, J. Chromatogr. B 664 (1995) 233–240.

[13] M.A. Fernandez, G. Carta, J. Chromatogr. A 746 (1996) 169–183.

[14] M.A. Fernandez, W.S. Laughinghouse, G. Carta, J. Chromatogr. A 746 (1996) 185–198.

[15] L.E. Weaver, G. Carta, Biotechnol. Progr. 12 (1996) 342–355.

[16] D. Farnan, D.D. Frey, C. Horvath, Biotechnol. Progr. 13 (1997) 429–439.

[17] E. Hansen, J. Mollerup, J. Chromatogr. A 827 (1998) 259–267.

[18] P.R. Wright, F.F. Muzzio, B.J. Glasser, Biotechnol. Progr. 14 (1998) 913–921.

[19] A.G. Ogston, Trans. Faraday Soc. 54 (1958) 1754–1757.

[20] T.C. Laurent, J.A. Killander, J. Chromatogr. 14 (1964) 317–330.

[21] R.I. Cukier, Macromolecules 17 (1984) 252–255.

[22] R.K. Lewus, G. Carta, AIChE J. 45 (1999) 512–522.

[23] V. Kapur, J.C. Charkoudian, S.B. Kessler, J.L. Anderson, Ind. Eng. Chem. Res. 35 (1996) 3179–3185.

[24] R.K. Lewus, F.H. Altan, G. Carta, Ind. Eng. Chem. Res. 37 (1998) 1079–1087.

[25] H.R. Mahler, E.H. Cordes, Biological Chemistry, Harper and Row, New York, 1966.

[26] R. Krishna, J.A. Wesselingh, Chem. Eng. Sci. 52 (1997) 861–911.

[27] T. Kataoka, H. Yoshida, Y. Ozasa, J. Chem. Eng. Japan 10 (1977) 385–390.

[28] H. Tsou, E.E. Graham, AIChE J. 31 (1985) 1959–1966.

[29] E.E. Graham, C.F. Fook, AIChE J. 28 (1982) 245–250.

[30] E.E. Graham, A. Pucciani, N.G. Pinto, Biotechnol. Progr. 3 (1987) 141–145.

[31] A. Shiosaki, M. Goto, T. Hirose, J. Chromatogr. A 679 (1994) 1–9.

[32] H. Yoshida, M. Yoshikawa, T. Kataoka, AIChE J. 40 (1994) 2034–2044.

[33] G.F. Bloomingburg, G. Carta, Chem. Eng. J. 55 (1994) B19–B27.

[34] D.M. Ruthven, Principles of Adsorption and Adsorptive Processes, Wiley, New York, 1984.